2nd International Symposium on Magnetic Beaing
July 12-14, 1990, Tokyo, Japan

REAL TIME BALANCING OF A FLEXIBLE ROTOR SUPPORTED BY MAGNETIC BEARING

Y. KANEMITSU , M. OHSAWA , K. WATANABE
EBARA RESEARCH CO.,LTD.
2-1 Hon Fujisawa 4-chome, Fujisawa-shi , 251 , JAPAN

Abstract

In this paper, the validity of a digital compensator of 5-axis magnetic bearing with a DSP for levitating a flexible rotor was confirmed by rotation test of the rotor operating beyond the bending natural frequencies of rotor.

After that, a real time balancing system was made, in which the digital compensator board with DSP for levitatig the rotor were employed and synchronous correction signals for balancing were synthesized by the DSP board to add to compensation signal and to cancel initial unbalance in the rotor. In a real time balancing test by using the combination of the analog and digital boards,the initial shaft vibration disappeared below the 1st bending critical speed. In another test, rotor vibration was suppressed under one tenth of initial value by the real time balancing using the digital compensator.

1 Introduction

A magnetic bearing which uses DC magnets and proxmity sensors measuring relative displacement between rotor and stator regulates magnet coil current to keep journal position constant and suppress rotor vibration. However it is difficult to make loop gain of it's controller larger because of the occurence of unstable vibration of levitated rotor, so that the shaft vibration caused by unbalance in rotor remains.

We have made a five axis active magnetic bearing as an experiment and controlled it by using an analog circuit and a digital IIR filter circuit as compensator in order to levitate a flexible rotor[1].

A digital compensator is suitable for adaptive or optimal control of a magnetic bearing because the properties of the compensator can be easily changed by modification of it's software. Real time balancing test of the rotor is carried out by using the digital compensator. The effective coefficient method is employed for the balancing, where effictive coefficient between a control signal from the compensator and sensor output is automatically estimated by a host personal computer.

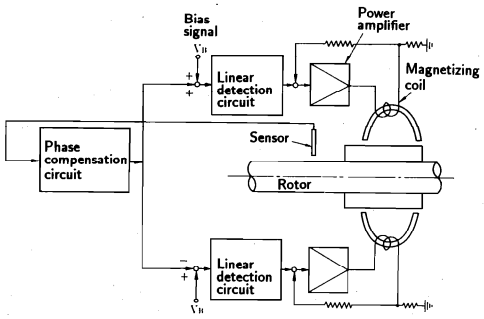

Fig.1 Block diagram of the rotor-AMB system

2 Test apparatus

2.1 Configuration of controller

Each axis of the active magnetic bearing(AMB) is regulated individually and it's controller is made up of a shift circuit of a displacement signal, a compensation circuit, two driver circuit and two power amplifiers. The block diagram of the system is shown in fig.1.

2.2 Rotor

Fig.2 shows a test apparatus for attesting the ability of the analog compensator and the digital compensator to levitate and balance a flexible rotor. The shaft is 531mm in length, and 26mm in maximum diameter. A induction motor rotor

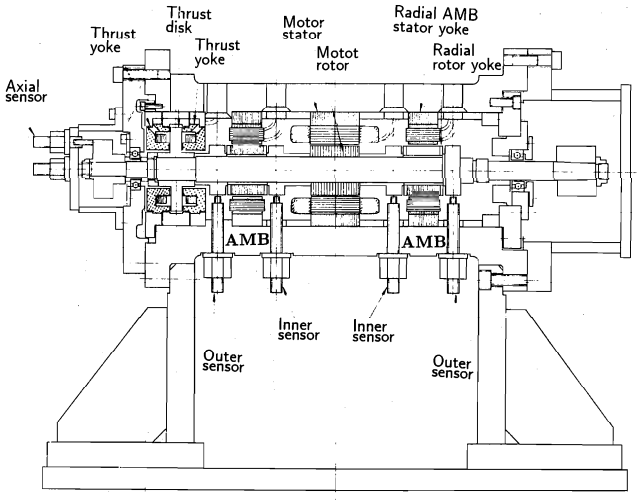

Fig.2 Test apparatus

is located in the middle of the shaft and two radial magnetic bearing(RMB) are situated on both sides of the motor rotor. A thrust magnetic bearing(TMB) is located at left end of shaft. Eddy current type proximity sensors with two mounting holes are prepared for the RMB sensors at both sides of the bearing, but inner sensors are used in tests. The natural frequencies and modes of the tested rotor was measured in a free-free condition and the measured results are presented in fig.3. The 1st and 2nd natural frequencies of the rotor were 290Hz and 690Hz, but in the real-time balancing test the 1st and 2nd natural frequencies became 340Hz and 760Hz respectively, because of modifying shapes of an unbalance disk attached at right end of the shaft and a sensor disk attached at left end of the shaft between rotation tests and balancing tests for the purpose to get a synchronous reference sine wave.

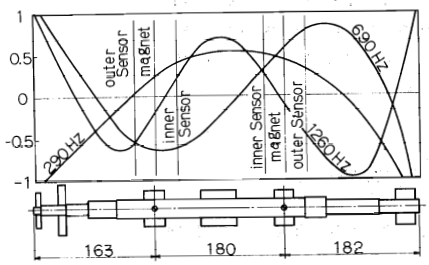

Fig.3 Natural frequencies and modes

2.3 Control using with analog compensator

For an analog compensator, a compensation circuit(A) containing a low-pass filter at high-frequencies and ones(B) without it were made and their measured transfer functions are as shown in fig.4.

In case of the rotation test using the analog compensator(A), the rotor reached 32,000rpm, but 1st natural vibration occured at this speed.

Fig.5 shows results of a rotating test using the compensator(B) which has a larger phase-lead than compensator(A) as shown in fig.4. The rotating speed reached 40,000rpm by compensator(B) without unstable vibration because of the increase in phase-lead. Maximum rotating speed in a series of ratating tests is 40,000rpm which is just below the second bending critical speed of 42,000rpm. As each test has no rigid mode resonance, and small resonance of 1st bending mode, we proved that the analog compensator has sufficient damping action in these frequency ranges.

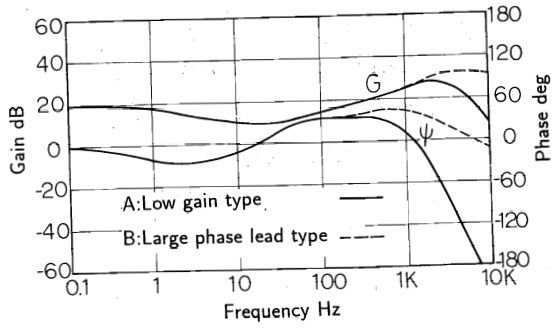

Fig.4 Transfer functions of analog compensators

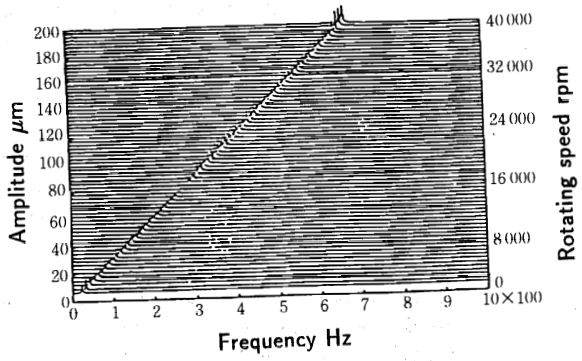

Fig.5 Waterfall diagram of rotating test [with analog compensator(B)]

2.4 Digital compensator with DSP

Based on an analog compensator(B) where the speed was raised beyond the 1st bending natural frequency of the rotor, an digital IIR filter compensator was prepared. The analog compensator must have parts on board changed when it is necessary to change their filter characteristics. With digital compensators, their filter characteristics are altered by changing contents of a filter coefficient memory. Therefore an optimal or adaptive control may be realized if it is possible to change the memory contents during operation.

When the transfer fanction G(s) on s-plane is given, the transfer function D(z) on z-plane is found by the bilinear transformation[2,3] expressed below.

$$D(z) = G(s)\big|_{s=\frac{2(1-z^{-1})}{\Delta T(1+z^{-1})}} \tag{1}$$

Where ΔT is the sampling period. As the relation between input $X(z)$ and output $Y(z)$ of n stages 2nd order IIR filter can be expressed as follows,

$$\frac{Y(z)}{X(z)} = D(z) = \prod^{n} \frac{b_0 + b_1 z^{-1} + b_2 z^{-2}}{1 + a_1 z^{-1} + a_2 z^{-2}} \tag{2}$$

The filter output $Y(z)$ can be found by calculating the output of each stages sequentially. The output $u(n)$ of each stage at $t = n\Delta T$ is found as follows:

$$\begin{aligned} u(n) &= b_0 e(n) + b_1 e(n-1) + b_2 e(n-2) \\ &\quad -a_1 u(n-1) - a_2 u(n-2) \end{aligned} \tag{3}$$

Fig.6 shows a block diagram of the digital compensator. A digital signal processor(DSP TI/TMS320C25) is used to implement the IIR filter type compensator which carrys out the equation(3). With this DSP, a high-speed 12-bit A/D con-

verter, of which conversion time is 2μsec, and three 12-bit D/A converters were used to make 3 compensators consisting of 7 stages 2nd-order IIR filters. The sampling frequency is 4000Hz for each axis (12kHz in total) at an instruction time of 125ns. A host personal computer(HPC) controls transference of data between the DSP and the HPC through a programmable peripheral interface (PPI μPD71055) and estimates unbalance of the rotor. The AMB system with this filter shown in fig.7 converts analog signals from the proximity sensors to digital signals by the A/D converter and stores them in the data memory on the DSP board . It also changes the compensated digital signals to analog signal for output by the D/A converter.

A comparison between transfer functions of analog and digital filter are shown in Fig.8. An IIR filter(1) is designed to have the same properties as the analog compensator(B) and an IIR filter(2) has an additional 2nd order phase lag-lead stage. The gain G of IIR filter(1) agrees with the analog compensator up to 700Hz. Beyond this frequency, however, the gain of filter(1) increases and fall abruptly beyond a certain frequency. In order to attain an adequate phase lead at 1st and 2nd bending natural frequencies of the rotor, another IIR filter(2) was made by adding a 2nd order phase lag-lead stage to the IIR filter(1).

2.5 Control using digital compensator

With the IIR filter(2) whose phase for the range including the natural frequencies of the rotor is advanced sufficiently as shown in fig.8, a waterfall diagram of radial vibration in the rotation test was attained as shown in fig.9. As the result the response is fully damped even at the bending critical speed 18,000 rpm. This means that the vibration of the rotor is fully controllable by means of the phase compensation. With this filter the speed was raised to 28,000rpm.

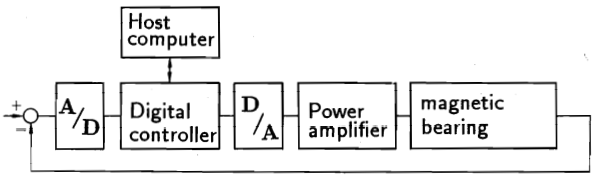

Fig.7 AMB system with the digital compensator

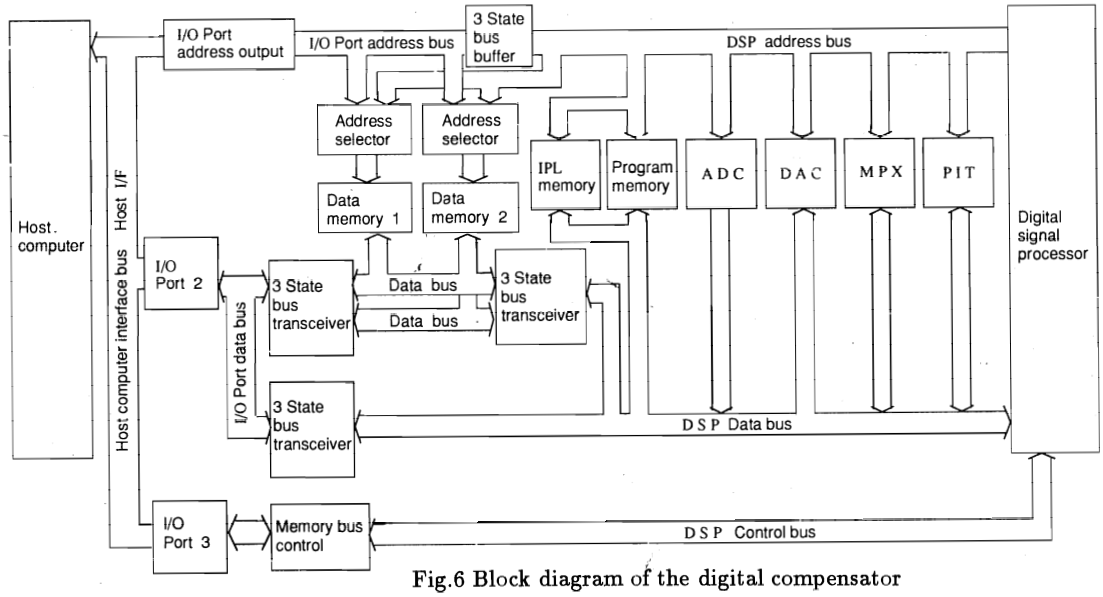

Fig.6 Block diagram of the digital compensator

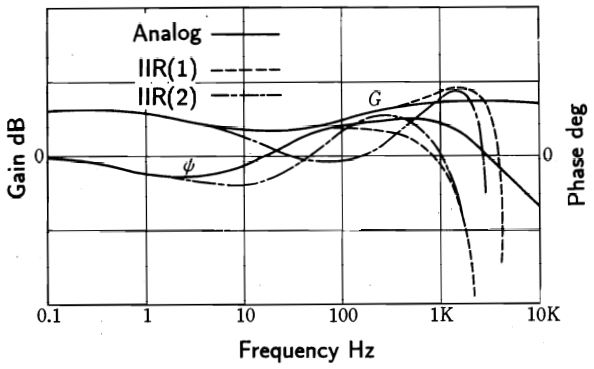

Fig.8 Comparison between the transfer function of analog and digital filters

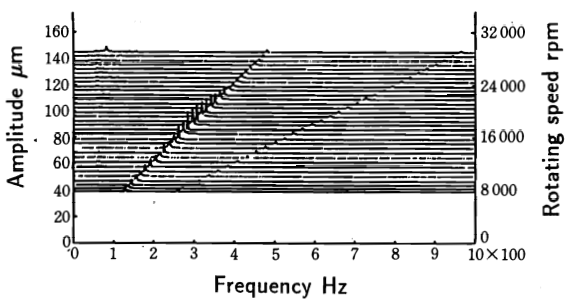

Fig.9 Waterfall diagram [with IIR filter(2)]

3 Method of real time balancing

In fig.10 which shows a block diagram of AMB-rotor system whirled by disturbance from mass unbalance, we attempt to suppress the vibration caused by unbalance disturbance $Fux(, Fuy)$ by adding a correction signal $Wx(, Wy)$, which synchronizes with rotating speed, to the compensation signal for levitating the rotor at an entrance of power amplifier in the way that the correction signal cancels the unbalance disturbance.

If we know a transfer function between synchronous correction signal and sensor output $G(s) = X/W_x$, we can easily get control input W_x by dividing sensor output by the transfer function $G(s)$. But it is very difficult to measure the transfer function at rotating frequency during rotation by a serbo analyser owing to the existance of synchronous vibration by unbalance.
Therefore we attempt to balance the rotor in almost the same way as so-called "effective coefficient method" employed in the field of balancing turbomachinery rotor as follows:

1. Trial inputs W_{xj}, W_{yj} meeting following equations are added to output signals of orthogonal compensators in the DSP according to a command from the HPC on the basis of the reference sine wave made by a eccentric disk attached at left end of the rotor.

$$W_{xj} = -W_j \cos(n\omega\Delta T + \theta_j) \quad (4)$$

$$W_{yj} = -W_j \cos(n\omega\Delta T + \theta_j + \pi/2) \quad (5)$$

where j is bearing number and ΔT is sampling period (1/4,000 sec).

2. Initial sensor outputs X_{k0}, Y_{k0}(k is sensor number) without the trial inputs and sensor outputs X_{kj}, Y_{kj} with the trial inputs W_{xj}, W_{yj} are written into memory on the DSP once and transfered from the DSP memory to the HPC memory.

3. Effective coefficients $a_{11} \ldots a_{42}$ between the trial inputs W_{xj}, W_{yj} and sensor outputs X_{kj}, Y_{kj} are calculated by the HPC as follows:

$$a_{1j} = \frac{\hat{X}_{1j}\exp(i\theta_{x1j}) - \hat{X}_{10}\exp(i\theta_{x10})}{\hat{W}_j \exp(i\theta_j)} \quad (6)$$

$$\vdots$$

$$a_{4j} = \frac{\hat{Y}_{2j}\exp(i\theta_{y2j}) - \hat{Y}_{20}\exp(i\theta_{y20})}{\hat{W}_j \exp(i\theta_j)} \quad (7)$$

where $\hat{X}_j, \theta_j$ are amplitude and phase of X_j respectively.

4. Amplitude W_j and phase θ_j of correction inputs W_{xj}, W_{yj} to correct the unbalance of rotor are estimated by the method of least squares and sent back to the DSP. Replacing a correction input vector $\mathbf{W}$, a initial sensor output vector $\mathbf{X}$,an effective coefficients matrix $\mathbf{A}$ and a residual vector $\mathbf{E}$ as follows:

$$\mathbf{W} = -[W_1 \exp(i\theta_1), W_2 \exp(i\theta_2)]^T \quad (8)$$

$$\mathbf{X} = [\hat{X}_{10}\exp(i\theta_{x10}), \hat{Y}_{10}\exp(i\theta_{y10}), \hat{X}_{20}\exp(i\theta_{x20}), \hat{Y}_{20}\exp(i\theta_{y20})]^T \quad (9)$$

$$\mathbf{A} = \begin{bmatrix} a_{11} & a_{12} \\ \vdots & \vdots \\ a_{41} & a_{42} \end{bmatrix} \quad (10)$$

$$\mathbf{E} = \mathbf{X} - \mathbf{A}\mathbf{W} \quad (11)$$

We obtain the correction input vector $\mathbf{W}$ on condition that $\mathbf{E}^T\mathbf{E}$ is minimized as follows:

$$\mathbf{W} = -(\mathbf{A}^T\mathbf{A})^{-1}\mathbf{A}\mathbf{X} \quad (12)$$

5. Synchronous correction inputs W_{xj}, W_{yj} to correct the unbalance are added to output signal of each compensator in the same way as 1..

First, the trial input Wx is added at output of compensator of each bearing controller and sensor output is measured . The measured signal is transfered from the DSP memory to the HPC while the rotor is rotating . A effective coefficient between the input W_x and the sensor output signal X is calculated by the HPC and amplitude and phase of correction signal W_x are determined .

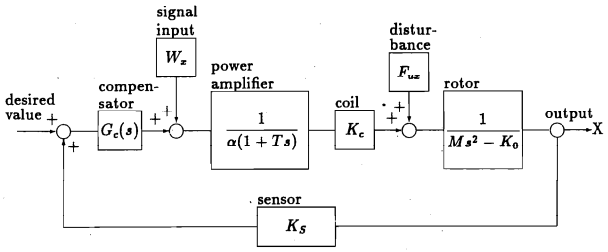

Fig.10 Block diagram of real time balance system of rotor levitated by AMB and whirled by unbalance

4 Method to make correction signals

Fig.11 shows a block diagram for explaining how to make the correction signals to compensate the unbalance of rotor by the DSP board and the HPC.
A procedure to make the signals is as follows:

1. The proximity sensor measures motion of the eccentric rotating disk attached at the left end of shaft and produces a reference sine wave. We employ phases between the vibration waveform the reference sine wave in the calculation of the effective coefficients to minimize a measurement error of phase.

2. A pulse signal per shaft rotation to trigger A/D conversion on is formed from the reference sine wave.

3. The number of system clock pulses(4MHz) during a rotation is counted by a PIT(Programmable Interval Timer, μPD71054) of which trigger signal is the pulse signal and is written in the data memory on the DSP board.

4. At the same time, the reference sine signal and the shaft vibrations are sequentially converted to digital signals by

the A/D converter, whose sampling frequency is 4KHz per channel, and 512 sampling data of each signal are kept in the memory.

5. The HPC communicates with the DSP board and reads the sampled data and the PIT data.

6. The HPC calculates fourier coefficients a, b of synchronous component with rotation of shaft as follows:

$$a = \frac{1}{256}\sum_{i=0}^{511} X(i)\cos(i\omega\Delta T) \tag{13}$$

$$b = \frac{1}{256}\sum_{i=0}^{511} X(i)\sin(i\omega\Delta T) \tag{14}$$

$$A = \sqrt{a^2+b^2}, \theta = \arctan(-b/a) \tag{15}$$

where $X(i), \omega, \Delta T, A$ and θ are sampled data, rotating speed, sampling period, amplitude and phase.

7. The calculated phases of shaft vibrations are corrected by subtracting the phase of the reference sine wave from them.

8. The synchronous correction inputs W_{xj}, W_{yj} to correct the unbalance calculated by the method based on the foregoing paragraph

9. The HPC communicates with the DSP board and writes the amplitude A and phase θ of synchronous correction input in the DSP memory.

10. A map of cosine values of each 2 degrees is prepared in the DSP memory beforehand.

11. The PIT measures a rotation period T and lapse time t from a last trigger pulse and the DSP calculates signal phases ψ_x, ψ_y of W_x, W_y based on the above-mentioned data as follows:

$$\psi_x = (\frac{2\pi t}{T} + \theta)\frac{180}{\pi} \tag{16}$$

$$\psi_y = (\frac{2\pi t}{T} + \theta)\frac{180}{\pi} + 90 \tag{17}$$

12. The correction values W_x, W_y are calculated by seeing the above-mentioned map of cosine values as follows:

$$W_x = A\cos\psi_x \tag{18}$$

$$W_y = A\cos\psi_y \tag{19}$$

13. The correction signals W_x, W_y are put out by the 12-bit D/A converters.

14. The process 11-13 are repeated every sampling.

Some waveforms of X and Y direction synthesized in the process 1-13 are shown in fig.12. In the case of low rotating speed, the synthesized waveform is smooth sine wave. But on the other hand the waveform becomes steped form of the sampling period 4000Hz when rotating speed is relatively high.

At first we employed the analog compensator for levitating the rotor and DSP board for balancing respectively. Secondly we used the DSP board for levitating and balancing the rotor.

5 Result of real time balancing

Fig.13 shows a system block diagram where we employed the analog compensator for levitating the rotor and DSP board for balancing respectively. Each of three known unbalances(3.2 , 4.5 , 27.9mmgr) is attached to the right end disk to change the unlabance of rotor and the rotor is raised to a prescrived speed. After that the real time balancing circuit was turned on and off sequentially and rotor vibrations at sensors of AMB were measured by FFT analyser and shown in fig.14-fig.18.

In fig.14, ordinate, abscissa and tilted co-ordinate represent amplitude of shaft vibration, frequency and time respectively when a smallest unbalance was attached and real time balancing was performed. At 10,000rpm initial synchronous vibration of 5μm almost vanished when the switch of the balancing circuit was on and again appeared when it was off. Vibration components except the synchronous vibration were not affected by this operation of the balancing. Waveforms of correction input and shaft vibration at 10,000rpm are shown

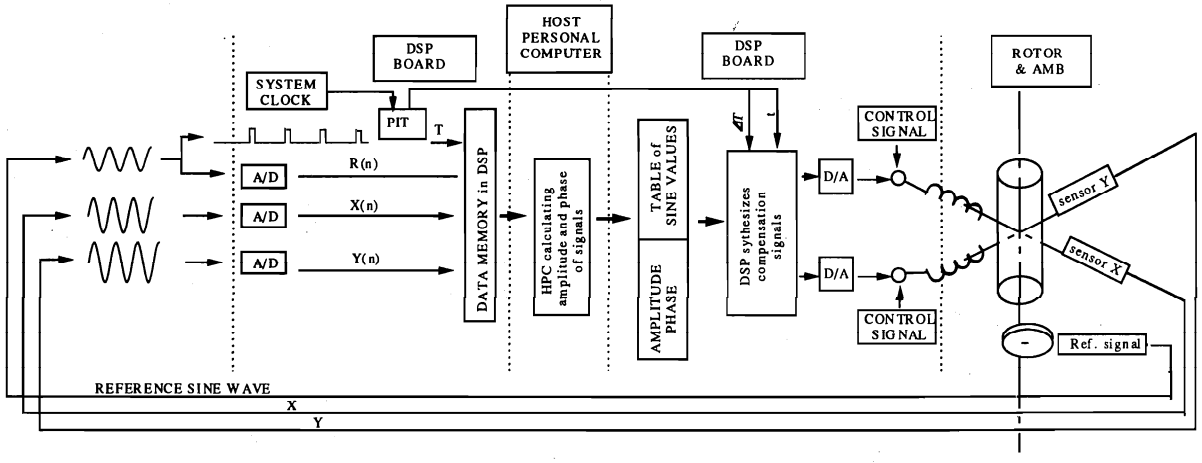

Fig.11 A block diagram for explaining how to make the correction signals

in fig.15. This figure shows that the correction input made by the DSP has the same period as the shaft vibration under balancing.

Near 1st bending critical speed(21,000rpm), initial vibration of 10μm decreases to 2μm under balancing in fig.14(b). Fig.16 shows waveforms of correction input and shaft vibration at 1st bending critical speed(21,240rpm). The correction input waveform becomes steped form of a sampling period ΔT because of high rotating speed.

Under executing the real time balance, initial vibration of 6μm decreases merely to 4μm at 30,000rpm and initial vibration does not change at 40,000rpm in fig.14(c)(d). Because impedance of the magnetizing coil of AMB bacomes large and the coil current are restricted to flow as the rotating speed increases, it is essential for improving the ability of the balancing to make the electric power source of the AMB larger or to make the coil impedance smaller .

Fig.17,18 show shaft vibration response where the attached unbalance became larger. The initial vibration remains at 21,000rpm in the case of 4.5mmgr, and the shaft vibration does not decrease at 15,000rpm in the case of 27.9mmgr. If we prepared a larger power source for the AMB, a large initial unbalance of rotor would be balanced even at high speed by the proposed method.

Next,we levitated and balanced the rotor only by the DSP board. A system block diagram in this case is shown in fig.19 and waveforms of shaft vibration and control signal at 10,000rpm is presented in fig.20.

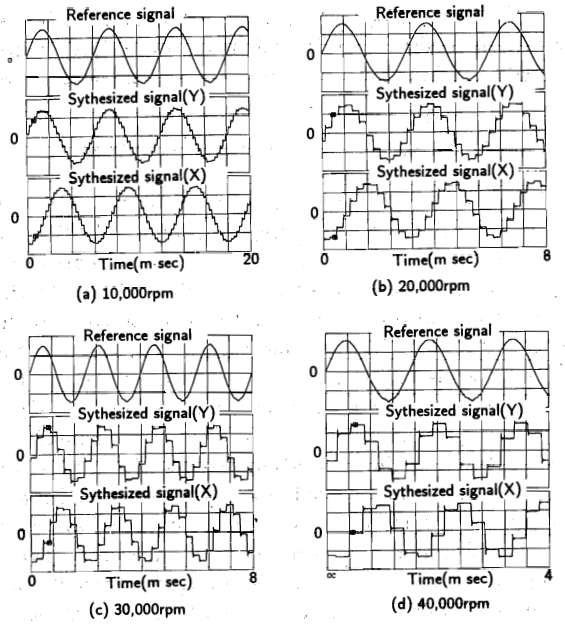

Fig.12 Synthesized waveform by DSP board

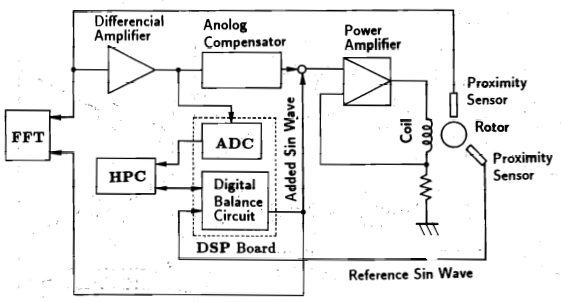

Fig.13 Block diagram of a hybrid system with an analog compensator and a digital balancing board

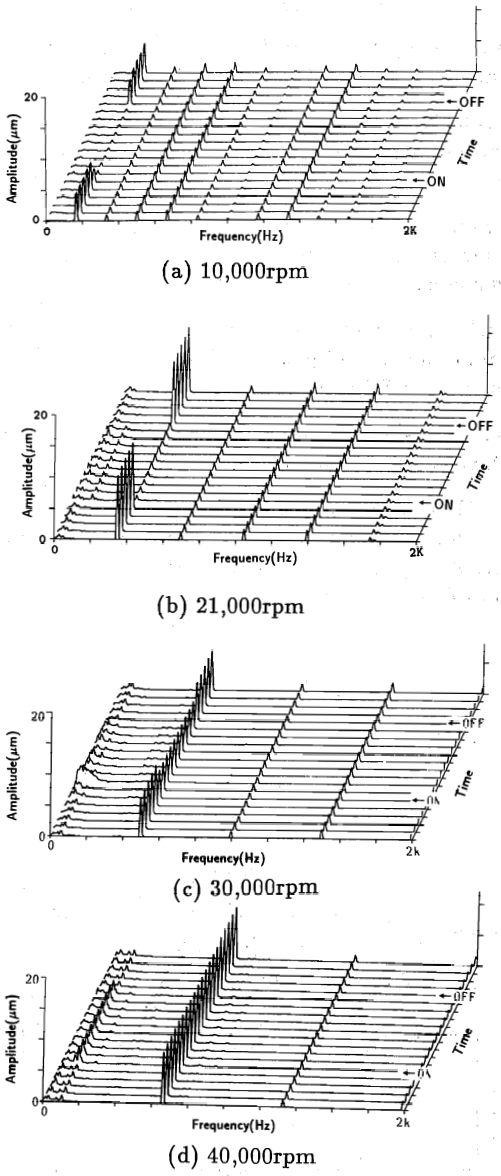

Fig.14 Waterfall diagrams of shaft vibration under balancing (unbalance=3.2mmgr)

According this test result, the shaft vibration under executing real time balance is one fifth of the vibration before balancing and the control signal supplied to the power amplifier under balancing is larger than that before balancing .

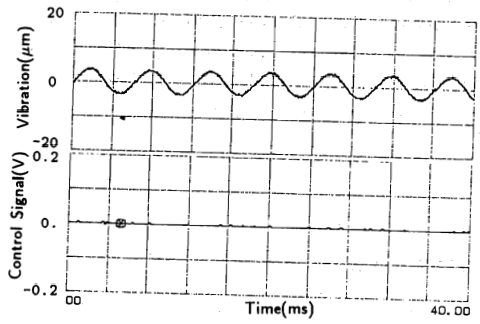

(a) before balancing

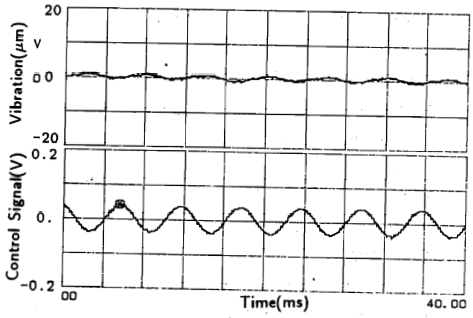

(b) under balancing

Fig.15 Waveforms of correction input and shaft vibration at 10,000rpm

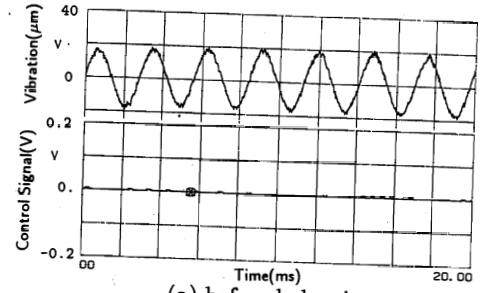

(a) before balancing

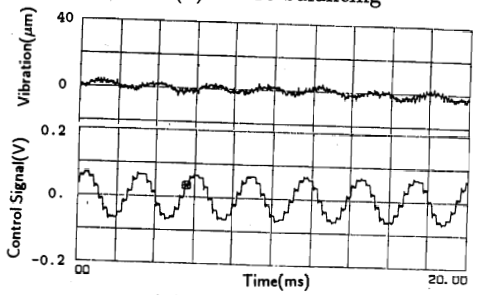

(b) under balancing

Fig.16 Waveforms of correction input and shaft vibration at 1st bending critical speed(21,240rpm)

From this test it become clear that the active magnetic bearing with digital controller is powerful actuator for balancing, especialy in the case that unbalance of a rotor changes while running.

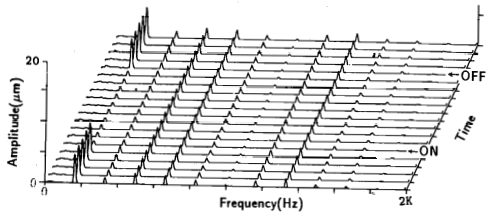

(a) 10,000rpm

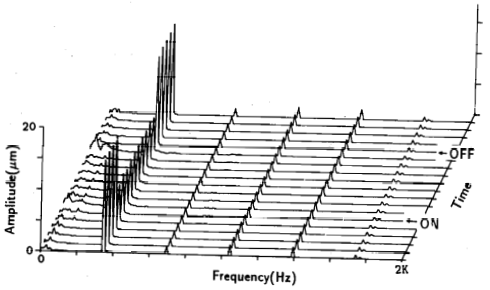

(b) 21,000rpm

Fig.17 Waterfall diagrams of shaft vibration under balancing (unbalance=4.5mmgr)

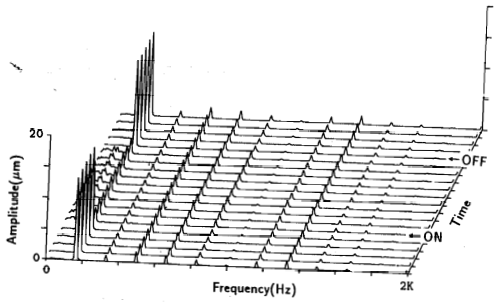

(a) 10,000rpm

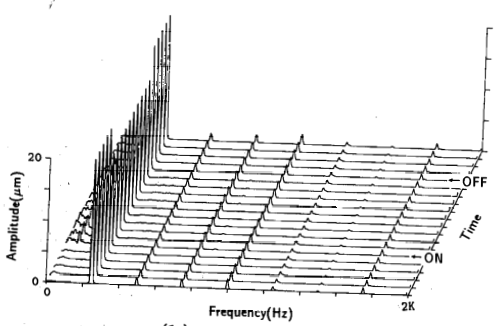

(b) 15,000rpm

Fig.18 Waterfall diagrams of shaft vibration under balancing (unbalance=27.9mmgr)

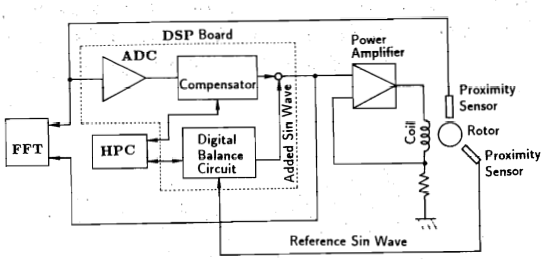

Fig.19 Block diagram of a system with DSP board for levitatig and balancing

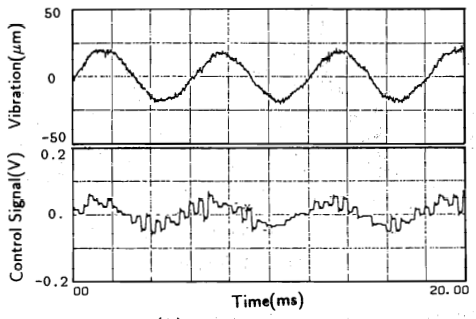

(a) before balancing

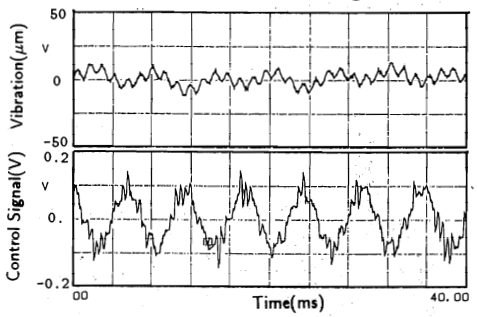

(b) under balancing

Fig.20 Waveforms of correction input and shaft vibration at 10,000rpm

6 Conclusion

We have made a real time balancing system in which the digital compensator board with DSP for levitatig the rotor are employed and synchronous correction signals for balancing are synthesized by the DSP board to add to compensation signal for levitation and to cancel initial unbalance in the rotor. In a real time balancing test by using the combination of the analog compensator and digital boards, the initial shaft vibration disappeared below the 1st bending critical speed.

In another test using only DSP board for levitating and balancing the rotor, the initial vibration was balanced by the DSP system at 10,000rpm.

7 References

[1] Kanemitsu,Y.,Ohsawa,M.,Watanabe,K. *Active Control of a Flexible Rotor by an Active Magnetic Bearing* Proc. 1st International Sympsium on Magnetic Bearings pp367-380(1988)

[2] Slivinsky,C.,Borniski,J. *Digital Signal Applications with TMS320 family* (Texas Instruments) pp689-724(1986)

[3] Kido,K. *Introduction to Digital Signal Processing* (in japanese) pp183-189 Maruzen(1985)

8 Nomenclature

a_{ij}	effective coefficient
$\mathbf{A}$	effective coefficient matrix
$D(z)$	transfer function on z-plane
$\mathbf{E}$	residual vector
F_{ux}, F_{uy}	unbalance disturbance
$G(s)$	transfer function on s-plane
j	actuater number
k	sensor number
ΔT	sampling period
W_x, W_y	correction input
T	rotating period
$\mathbf{W}$	correction input vector
X, Y	relative displacement
$\mathbf{X}$	initial vibration vector
θ	phase
ψ_x, ψ_y	phase of correction input
ω	rotating speed